Adapting Robot Paths for Automated NDT of Complex Structures using Ultrasonic Alignment

Jonathan Riise[1,a)], S. Gareth Pierce[1], P. Ian Nicholson[2], Ian Cooper[2] and Carmelo Mineo

[1]Centre for Ultrasonic Engineering, Department of Electronic and Electrical Engineering, University of Strathclyde, 204 George Street, Glasgow, UK
[2]TWI Technology Centre Wales, Harbourside Business Park, Harbourside Road, Port Talbot, UK

a)Corresponding author: jonathan.riise@strath.ac.uk

Abstract. Automated inspection systems using industrial robots have been available for several years. The IntACom robot inspection system was developed at TWI Wales and utilises phased array ultrasonic probes to inspect complex geometries, in particular aerospace composite components. To increase inspection speed and accuracy, off-line path planning is employed to define a series of robotic movements following the surface of a component. To minimise influences of refraction at the component interface and effects of anisotropy, the ultrasonic probe must be kept perpendicular to the surface throughout the inspection. Deviations between the actual component and computer model used for path-planning result in suboptimal alignment and a subsequent reduction in the quality of the ultrasonic echo signal.

In this work we demonstrate methods for using the ultrasonic echo signals to adapt a robotic path to achieve a minimal variation in the reflected surface echo. The component surface is imaged using phased array probes to calculate a sparse 3D point cloud with estimated normal directions. This is done through a preliminary alignment path covering approximately 25% of the total surface to minimise the impact on overall inspection time. The data is then compared to the expected geometry and deviations are minimised using least-squares optimisation. Compared to manual alignment techniques, this method shows a reduction in surface amplitude variation of up to 32%, indicating that the robot is following the surface of the component more accurately.

INTRODUCTION

In recent years there has been a trend in using industrial robots for Non-Destructive Testing (NDT) of complex shaped parts [1–3]. This is primarily a consequence of the uptake of composite components being increasingly used in the aerospace industry since the early 2000s. These components exhibit highly curved geometries which are difficult to inspect with traditional automated methods such as gantry systems [4]. Industrial robots offer several advantages in this regard due to their ability to follow complex paths, manipulate NDT probes with six Degrees of Freedom (DoF) and scan at speeds of up to several meters per second. Furthermore, industrial robots are flexible tools which can quickly be adapted to different inspection scenarios and are relatively inexpensive due to their widespread use in other industries.

TWI and the University of Strathclyde have researched new ways of deploying industrial robots for the ultrasonic inspection of complex aerospace structures. The IntACom inspection cell at TWI's facilities in South Wales is shown in FIGURE 1 and consists of two KUKA KR16-L6 industrial robots capable of inspecting a volume of approximately 5m^3. The two robots can either work independently for pulse-echo inspections or cooperatively for through-transmission inspections. The system uses water jet nozzles containing either phased array or single-crystal probes to provide ultrasonic coupling to components being inspected. The project began in 2012 as a collaboration between TWI, Rolls-Royce, GKN and Bombardier and is now in its third development phase.

FIGURE 1. The IntACom robotic inspection system at TWI Technology Centre Wales

There is an increasing interest in furthering the Technology Readiness Levels (TRL) of automated inspection systems and making these systems more adaptable to changes such as variations in part positioning. Some of the key challenges include increasing the positional accuracy of industrial robots, integrating NDT hardware, raising the level of automation, visualising data in 3D and optimising trajectory planning for NDT. Trajectory planning is currently done off-line in a virtual environment using Computer Aided Design (CAD) models. The resultant NDT paths are defined relative to a datum on a CAD model which is subsequently identified during the actual setup. Identifying a component and its exact pose (position and orientation) with respect to a robot is a significant challenge to obtaining a more flexible system. This step is traditionally performed by manually driving the robot to the part, a process which is time-consuming and prone to operator error. Alternatively, an optical sensing system can be used, but this requires a change of robot tool and can be expensive. Current research at TWI has shown that it is possible to perform high-accuracy alignment between the component and robot coordinate frames using ultrasonic Time-of-Flight (ToF) information. The focus of the current paper is to present a method wherein coordinate reference frame corrections can be automatically applied to increase the quality of ultrasonic NDT inspections.

TRAJECTORY PLANNING AND EXECUTION

Industrial robots can be controlled in several ways, the most common being with a "teach-pendant" which allows an operator to manually position and orient the Tool-Centre-Point (TCP) of a robot. Although this method is sufficient for repetitive tasks such as pick-and-place operations, it is unfeasible for a human to accurately design an inspection path for components with complex surface geometries. Instead, CAD models are used to define a path where an ultrasonic probe is kept perpendicular to the surface at all times. An example path planning operation is shown in FIGURE 2a. Here, the tool centre point is defined as the centre of a water jet nozzle. Defining paths off-line allows an operator to optimise path parameters and check for collisions before the actual path is carried out. This approach, however, assumes that the virtual models and the positions of part and robots match the real world.
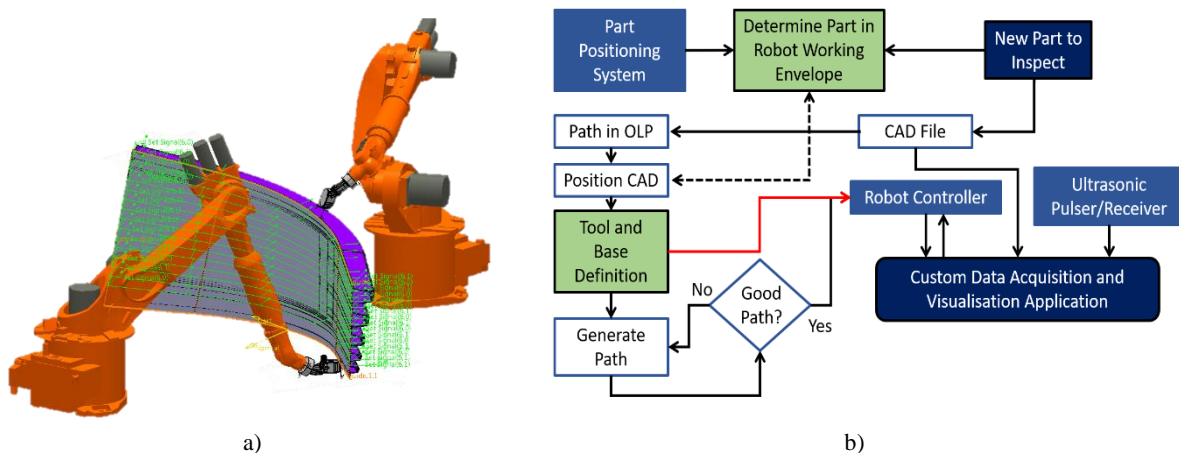

a)   b)

FIGURE 2. a) Off-line path planning application. b) Workflow highlighting the alignment step between the virtual and real robot environments

To avoid the need for modelling the entire robotic cell accurately, off-line paths are defined with respect to the component itself. This way, the part can be placed in any location where the robot can reach it and the path can be modified through updating a base coordinate reference frame specific to the robot. This step is highlighted in the overall inspection workflow, illustrated in FIGURE 2b. The IntACom system architecture is described in greater detail in [3]. The accurate definition of component pose is a crucial step in being able to execute an optimal NDT path where the TCP stays normal to the surface throughout. Any deviations from the normal will result in a suboptimal sonification of the part by the ultrasonic transducer.

Alignment Tolerances

To minimize influences of refraction at the component interface and effects of anisotropy, the ultrasonic probe must be kept perpendicular to the surface throughout the inspection. An experiment was conducted to determine the tolerances for probe alignment. A linear 5MHz phased array ultrasonic probe containing 64 elements, with a pitch of 0.6mm was rotated above the flat surface of a calibration block. A central sub aperture of 15 elements was used to match the probe elevation. To avoid collision, the water jet nozzle containing the probe is kept approximately 15mm above the surface of the part. The probe was rotated about the x and y directions (angles B and C shown in FIGURE 3a) and the amplitude of the front wall reflection was recorded at each angle increment. The rotation around the z axis (angle A) does not lead to a change in signal amplitude as the probe stays normal to the surface. Although the angle A was not changed, its value was recorded to ensure correct encoding of the collected ultrasonic data.
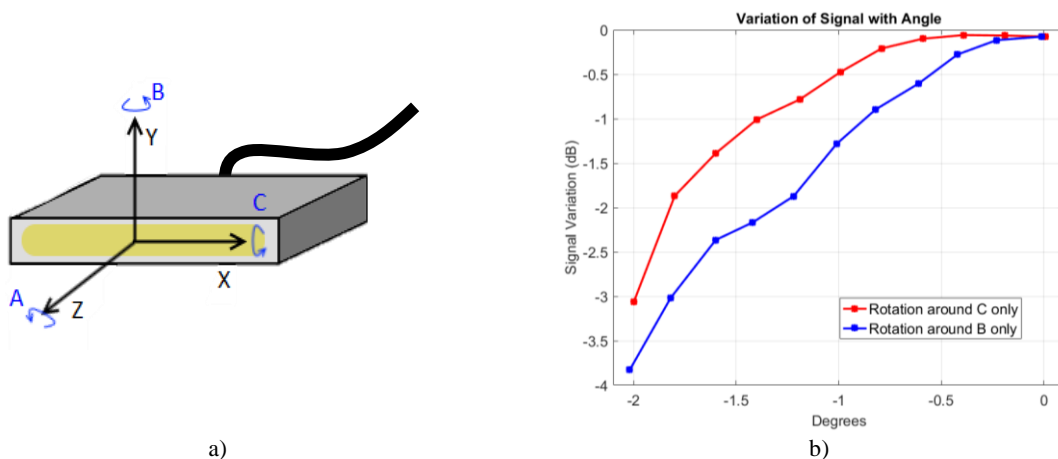

a)   b)

FIGURE 3. a) Coordinate system of a phased array probe. The origin is at the center of the probe face. b) Variation of signal amplitude with angles B and C.

The result of incrementing the probe from perpendicular (zero degrees) to -2 degrees in 0.2 degree steps is shown in FIGURE 3b. Positive rotations are not included due to the symmetry of the setup. It is evident that the rotation around B has a larger detrimental effect on the signal amplitude, which is expected from the probe geometry. The decrease in amplitude is even greater when the probe is misaligned in both axes, as shown in FIGURE 4. A limit of 2dB variation is tolerable in most inspection scenarios. As evident from FIGURE 4, this means the probe must be kept normal to the surface within ±1 degree. To obtain this level of accuracy it is crucial that the TCP of the ultrasonic probe and the part position and orientation are correctly calibrated. A method of ultrasonic probe calibration has previously been presented in [5]. Although it is important that the probe follows the surface at a specified distance to avoid collisions, this off-set distance has less effect on signal amplitude due to the relatively low attenuation of ultrasound in water.
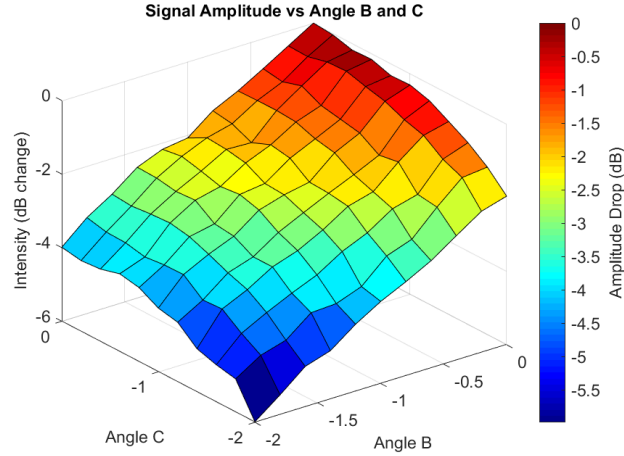
FIGURE 4. Surface representation of the amplitude drop as a function of probe misalignment along two axes.

Once the probe and part coordinate reference frames have been adequately calibrated, the scan can be executed. As shown in FIGURE 2b, the robot controller communicates with the ultrasonic pulser-receiver through a custom written software package. Ultrasonic data is encoded with robot feedback positions obtained through a server application which time-stamps both sets of information with a shared timer. Once gathered, the data is displayed in a 3D environment and overlaid on a CAD model of the component. The custom written software allows the simultaneous visualization of A-, B- and C-scan data to allow easy interpretation by the operator.

Part Positioning

Several established ways exist to determine the position of a part in a flexible, automated environment [7]. Primary methods are listed in TABLE 1, including the typically obtainable absolute accuracy.

TABLE 1. Methods for part positioning with associated accuracy.

Method	Accuracy	Comments
Optical scanning system (e.g. laser profiler)	Very high (< 50μm)	Time-consuming, needs dry surface and separate robot tool
Motion Capture System	Medium (1-2mm)	Expensive and extensive setup required. Line of sight needed.
Machine vision part recognition	Medium (0.5-5mm)	Controlled layout needed. Machine learning required. Line of sight needed.
Manual Methods	Medium (> 1mm)	Time consuming, prone to operator error
Ultrasonic alignment	High (< 1mm)	Needs initial alignment

Of the methods listed in Table 1, the optical scanning system gives the most precise results but can be expensive to implement. Machine vision techniques have successfully been implemented in highly controlled environments such as conveyor-belt type operations, but struggle with accurately determining the position of large components without sophisticated training algorithms [8]. Manual methods are operator-dependent and although cheap, drastically lower the automation level of the inspection process.

The developed method is only able to determine the exact alignment between part and robot if the robot can perform an initial surface scan of the part using an ultrasonic probe in a water jet nozzle. As such, a relatively accurate knowledge of the pose of a part is needed in order to commence scanning. This is possible to achieve using rigid fixtures and jigs, but these can be expensive and sacrifices flexibility. Furthermore, these types of fixtures are not economical for large-scale, low-volume manufactured goods which are expected to become the norm during the next industrial revolution [6]. TWI currently uses flexible jigs and fixtures which are manufactured through fused deposit modeling (also known as 3D printing) to repeatedly place parts to within a few millimeters of the expected position and orientation. The following section describes the method used in this work for accurately determining the pose of the part. The method, labelled ultrasonic alignment in Table 1, is based on the analysis of the time-of-flight variations in the reflected surface echo..

ULTRASONIC ALIGNMENT FOR PART POSITIONING

A visual representation of the developed method for alignment is shown in **FIGURE 5**. During the path planning process, several key points are selected which cover 10-30% of the part surface. To avoid collisions while moving between these key points, the robot follows the surface between each target location. The ultrasonic pulser-receiver is set up such that the front-wall echo is recorded at each location. After the scan finishes, the time-of-flight information encoded with robot positional data is used to create a point cloud representing the surface of the component (P_s). The key points identified during the path planning stage form another (sparser) point cloud, representing the CAD models expected position (P_{CAD}).

It should be noted that the method presented here resembles the method presented by the authors of [9]. The main differences in methodology are that this work uses a single calculation step, uses water nozzles and phased array probes as opposed to the immersion technique presented in [9]. To avoid an iterative algorithm, key points are determined more robustly, alleviating the need for an update loop. At each P_{CAD} key point, a search algorithm finds a set of P_S and fits a plane to the points. The normal vector, average time-of-flight and amplitude are then used to create a matched key point. A list of matching key points is created and the deviation between P_S and P_{CAD} can be calculated. This information is then transferred back to the robot controller to update the coordinate reference system for that inspection.
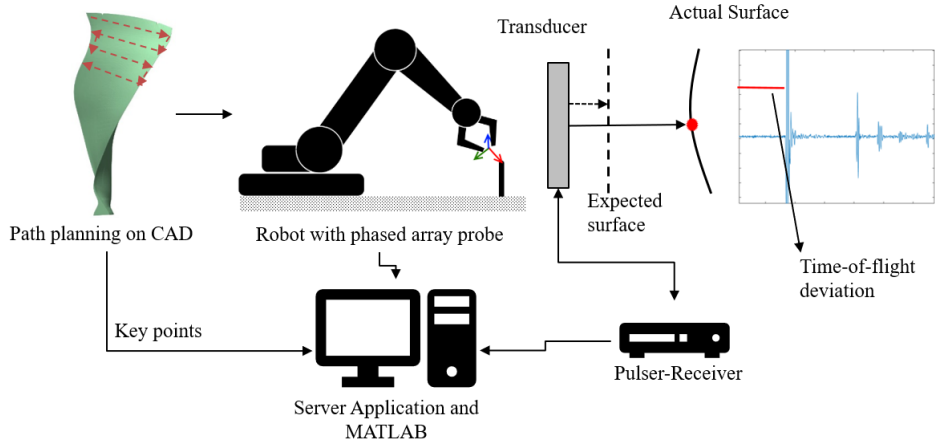

FIGURE 5. Illustration of the ultrasonic alignment technique

Matching Algorithm

Point cloud registration is a topic which has been around for many years [10] and the approach is generally to search for corresponding points in different models and find a rigid transformation which estimates pose deviation. One of the key challenges is to define which points correspond to one another. The current method avoids this problem by only considering points in a defined region of space around each key point. To ensure the data is adequate, two checks are performed on the data before a key point is generated from data in P_S. First, the average amplitude must be above a set threshold and secondly, the normal vector must be within a set tolerance.

For each key point in P_{CAD}, a specified volume is defined in 3D space and points, $\mathbf{P}_i = (P_{ix}, P_{iy}, P_{iz})^T$ from P_s which fall inside this volume in are used to calculate a single, corresponding, key point. The average amplitude of $\mathbf{P}_1 \ldots \mathbf{P}_N$, (where N is the number of points inside the volume) should be above a set threshold, dependent on the reference amplitude of the scan. If the average amplitude falls below this value, the key point is discarded from the list of key points in P_{CAD}.

The normal vector is calculated by finding the normal vector of a plane fitted to the data using a least-squares optimization. This is done by first removing the centroid of the subset of P_s and computing the Singular Value Decomposition (SVD) of the resulting coordinates, $\mathbf{Y} = \mathbf{U\Sigma V}^T$ where $\mathbf{\Sigma}$ is a 3x3 matrix wherein the diagonals correspond to the eigenvalues. The normal vector of the plane is then defined as the singular vector from $\mathbf{V}$ corresponding to the lowest eigenvalue. The normal vector for each plane is compared to the expected normal vector of the key point by taking the dot product of the two vectors. If the direction is too dissimilar, the key point is again discarded from the list in P_{CAD}.

If a set of points in P_{CAD} meet the above conditions, then a corresponding single point is created. The 3D coordinates of this matched key point are the average of the set of points in the chosen volume. In this way, the entire point cloud generated from the time-of-flight data does not need to be searched which improves the performance of the algorithm. Once all key points have been matched or discarded, the rigid transformation between the expected and observed points cloud is found through the algorithm described in [11]. First the centroids of each point set (K_{CAD} and K_S) is calculated and removed from their respective point sets, as shown in Equation 1.

$$K_{CAD} = P_{CAD} - \frac{1}{N}\sum_{i=1}^{N} P\,^i_{CAD} \qquad K_S = P_s - \frac{1}{N}\sum_{i=1}^{N} P\,^i_s \qquad (1)$$

The covariance matrix of the two sets is then given by Equation 2.

$$X_{3x3} = \sum_{i=1}^{N} K_{CAD}^i \cdot K_{Surface}^i \qquad (2)$$

SVD is then performed on $\mathbf{X}$ to obtain the factorization $\mathbf{U\Sigma V^T}$. The rotation matrix aligning the orientation of the point sets is then given by $\mathbf{R = UV^T}$. The 3x3 rotation matrix can then be represented as three Euler angles as expected by the KUKA robot control software. The translation vector (displacements in x, y and z) aligning the two sets is given by $\mathbf{T} = K_S\text{-}R*K_{CAD}$. The matching algorithm, implemented in Matlab 2016b, is represented as a flow chart shown in FIGURE 6.
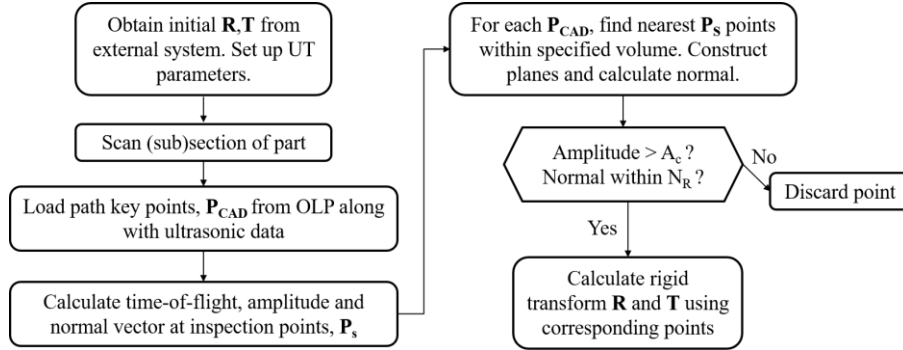

FIGURE 6. Flowchart illustrating the different matching steps. A_c and N_R are thresholds set at the beginning of the process.

The described method allows for the accurate alignment of robot trajectory and part based on a few assumptions. First, it is anticipated that the part is already close to the expected position such that the robot can move without collision and that the front-wall ultrasonic echo can be observed at all points. Secondly, the alignment scan may not be able to scan the entire surface, so if the part is invariant under translation and rotation the result for this degree of freedom may have to be ignored. Key features such as corners or fixturing holes would be ideal to use, but these can be difficult to accurately identify using a water-jet coupled ultrasonic probe. Finally, the curvature of the part must be sufficiently low so that a plane can be approximated at each P_{CAD} inspection point. In practice this means that P_{CAD} key points cannot include areas close to edges and corners.

RESULTS

An experiment was carried out in a controlled setting to test the accuracy of the developed approach. A flat plastic sample, measuring 150x100x10mm, machined to a tolerance of 0.1mm, was fixed in place in the robot's working envelope. The position and orientation of the sample was determined using a laser profiler. The sample was then ultrasonically scanned in a raster pattern with a 5MHz phased array probe, with a pitch of 0.6mm using an electronically scanned sub-aperture of 15 elements to match the elevation of the probe. Ultrasonic data was gathered using a Peak NDT Micropulse 5PA unit and encoded with the robot's positional information. The resulting scan is shown in FIGURE **7**b where it can clearly be seen that there is little variation in the front wall echo. The robot's reference frame was then changed such that a misalignment of 1.1mm in x, -0.7mm in y, 1mm in z, 0.2° about z, -0.8° about y and 0.5° about x was applied. These values were chosen to represent typical

misalignments seen in practice and are also shown in Table 2. The sample was then scanned again, as shown in Fig. 7b which clearly shows the variation in time-of-flight across the surface.
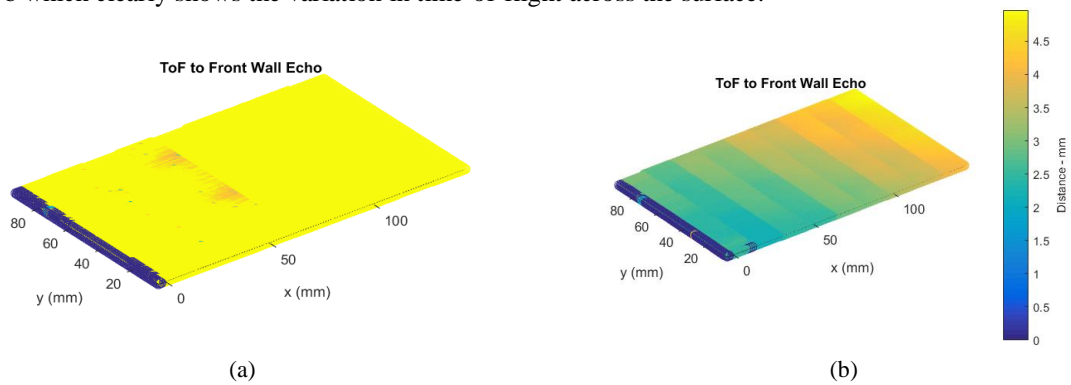

(a)   (b)

FIGURE 7. Reference scan of a flat sample. When the sample is well aligned (a), there is almost no variation in the ToF. When purposely misaligned (b), the ToF varies across the sample. The goal of the method is to calculate this misalignment.

After this second scan had been collected, the ultrasonic alignment algorithm was applied to the data to test how well the original calibration could be recovered. The calculated corrections are shown in Table 2. As evidenced in Table 2, the sample is invariant under transformation in x, y and around z and the corrected values are not usable. However, the results of the alignment algorithm for the remaining three dimensions are within 0.03mm and 0.02°.

TABLE 2. Applied and recovered misalignment data for a flat sample.
Angles A, B and C correspond to rotations about z, y and x.

Dimension	Applied Offset	Recovered Offset	Error
X	1.10 mm	0.25 mm	0.85 mm
Y	-0.70 mm	0.13 mm	-0.83 mm
Z	1.00 mm	0.97 mm	0.03 mm
A	0.2°	0.01°	0.19°
B	-0.8°	-0.82°	0.02°
C	0.5°	0.49°	0.01°

Complex Geometry Sample

Although the initial experiment provided good results, the simple geometry of the sample is not representative of most parts which are inspected using the IntACom system. Therefore, to test the algorithm further, it was used on a complex aero-foil shape provided by an industrial partner of TWI. The component's position and orientation were manually found by driving a metal spike mounted at the robot's TCP to a set of reference points. The component, measuring roughly 1.5m in height, was scanned using single-crystal 1MHz probes with a raster step of 2mm. The scan should aim at keeping the ToF distance within 1.5mm from the reference standoff distance. Due to the complex part geometry and mismatch between the CAD model and actual part, it was not possible to ascertain the pose with the laser profiler. Instead, a metric was defined to determine the quality of the ultrasonic scan. A reference front-wall echo signal of 50% full-screen height was set on a flat section of the component. Inspections covering the whole sample were then determined to be adequate if the variation of the front-wall echo remained within 2dB throughout the scan.

An alignment scan path was designed using off-line path planning to cover roughly 25% of the total surface of the component. This subsection was chosen as it would provide enough information to perform alignment while keeping the overall inspection time short. The scan was carried out and the alignment method described in this paper was applied to the acquired data. After applying the calculated corrections to the robot's base reference system, the entire component was scanned again. The variation in amplitude is shown in FIGURE 8. As mentioned, the component geometry was not entirely consistent with the CAD geometry, so the scan path included over-spray points at the edges. These points made up about 5% of the total number of inspection points and were removed for the variation analysis.
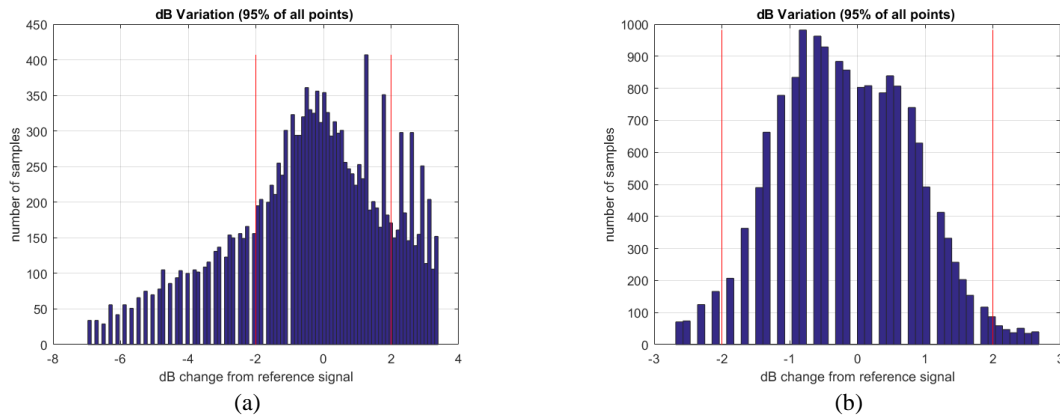
FIGURE 8. Variation in amplitude from a reference signal when scanning an aerospace component with a complex surface geometry. (a) shows the variation before the ultrasonic alignment method was applied while (b) shows the results after the alignment corrections were applied.

Figure 8a shows the variation in amplitude when the part was scanned only using manual alignment. The variation from the reference signal is between -7dB and 3.3dB and a range of 8mm was seen in the ToF data, with a standard deviation of 2.06mm. After the alignment was applied (Fig. 8b), the variation in signal amplitude was between 2.8dB and -2.7dB, though as evident from the graph, most of the inspection points are within the desired 2dB range. The variation range in ToF values was 3.7mm with a standard deviation of 0.76mm. As a measure of improvement, the average change in signal amplitude was 32.2% better after the alignment had taken place. These results underline the usefulness of the technique and its ability to provide high-accuracy alignment between the robot and part reference frames, even when scanning component which deviate from their CAD models.

FUTURE WORK

As the results from scanning a flat plate show, the alignment algorithm works best on components which are not translationally invariant. Future research will investigate ways to improve ultrasonically imaging reference points such as corners or edges of a component to provide stronger matching features. This could potentially help provide a better absolute alignment for all six degrees of freedom. Furthermore, it has been noted that components manufactured from Carbon Fiber Reinforced Polymers (CFRP) have a tendency to "spring-back" from their mold after curing. This means that a simple rigid-body transformation is no longer adequate as the trajectory designed on a CAD model will never match the geometry perfectly. Future work will look at methods of using non-rigid point cloud alignment methods to not only update the robot base reference data but the path itself as well.

CONCLUSIONS

A novel technique for aligning robot and part coordinate frames for automated ultrasonic NDT has been presented. The technique automatically applied coordinate reference frame corrections to increase the quality of ultrasonic NDT inspections. This work is specifically designed to aid in the flexible inspection of large aerospace components with complex surface geometries where the use of bespoke rigid fixtures and jigs is undesirable. The technique is a method of point-cloud registration based on key features established during the path planning phase of the inspection process. It was shown that the technique can correct for misalignments with sub-mm accuracy on simple geometries. The method was also used to improve the quality of a complex aerospace part inspection. This improvement in quality of up to 32% was demonstrated by comparing the variation in amplitude of the reflected surface echo as well as the time-of-flight variation. Future work will focus on adapting paths to components which do not conform to their CAD geometry.

ACKNOWLEDGEMENTS

REFERENCES

1. C. Mineo, C. MacLeod, M. Morozov, S.G. Pierce, T. Lardner, R. Summan, J. Powell, P. McCubbin, C. McCubbin, G. Munro, S. Paton, D. Watson, and D. Lines, IEEE Int. Ultrason. Symp. IUS **2016**–**Novem**, (2016).

2. E. Cuevas, M. López, and M. García, in *4th Int. Symp. NDT Aerosp.* (Berlin, Germany, 2012), pp. 1–12.

3. C. Mineo, S.G. Pierce, B. Wright, I. Cooper, and P.I. Nicholson, Insight - Non-Destructive Test. Cond. Monit. **57**, 161 (2015).

4. R. Bogue, Assem. Autom. **32**, 211 (2012).

5. J. Riise, L. Farr, M. Lindop, G. Pierce, P.I. Nicholson, and I. Cooper, in *12th Eur. Conf. Non-Destructive Test. (ECNDT 2018)* (NDT.net, Gothenburg, 2018), pp. 1–8.

6. R.H. Schmitt, M. Peterek, E. Morse, W. Knapp, M. Galetto, F. Härtig, G. Goch, B. Hughes, A. Forbes, and W.T. Estler, CIRP Ann. - Manuf. Technol. **65**, 643 (2016).

7. J.E. Muelaner and P.G. Maropoulos, Procedia CIRP **25**, 169 (2014).

8. M. Zhu, K.G. Derpanis, Y. Yang, S. Brahmbhatt, M. Zhang, C. Phillips, M. Lecce, and K. Daniilidis, 2014 IEEE Int. Conf. Robot. Autom. 3936 (2014).

9. H. Zhang, C. Xu, and D. Xiao, Proc. Inst. Mech. Eng. Part C J. Mech. Eng. Sci. **0**, 1 (2018).

10. P.J. Besl and N.D. McKay, IEEE Trans. Pattern Anal. Mach. Intel. **14**, 239 (1992).

11. K.S. Arun, T.S. Huang, and S.D. Blostein, IEEE Trans. Pattern Anal. Mach. Intell. **9**, 698 (1987).